

## NUMERICAL ANALYSIS AND OPTIMIZATION OF THERMAL PERFORMANCE OF LITHIUM BATTERY PACK BASED ON AIR-COOLING STRATEGY

by

**Yu HU\* and Bin MAO**

Foshan Xianhu Laboratory of the Advanced Energy Science and Technology Guangdong,  
Xianhu Hydrogen Valley, Foshan, China

Original scientific paper  
<https://doi.org/10.2298/TSCI210628023H>

*An effective and robust thermal management system can control the temperature of lithium batteries and maintain the long service life and high performance of the module. In this work, the thermal design and optimization of cylindrical battery packs based on air-cooled thermal management strategies are studied. Lumped model is implemented to investigate the thermophysical characteristics of single cell, and the experimental measurements is used to determine the transient heat generation of cylindrical lithium batteries under different discharge rates. On this basis, the CFD method is used to analyze the temperature of the battery pack, and the heat dissipation performance of the air-cooled heat management system is explored. Finally, different air cooling strategies are investigated by changing the area and position of inlet and outlet to obtain the best cooling scheme. The results indicate that the multi-inlet and multi-outlet structure in this paper can significantly lower the temperature and improve the temperature uniformity in the battery pack. A better air-cooling performance can be obtained under the optimal parameter configuration, which will help the design of the air-cooled battery thermal management system.*

**Key words:** *air cooling strategy, battery thermal management, parameter optimization, CFD*

### Introduction

In recent years, the demand all over the world for energy resources has been increasing, which has caused serious environmental pollution and aggravated the global warming. The primary energy consumption in the world is fossil fuels, and the part of fossil fuels used in the transportation industry accounts for 49% [1, 2]. In order to conserve energy and protect environment, green energy power and clean vehicles have become the main development direction of the automobile industry [3]. Lithium batteries have high energy density, high power density and long service life, which are usually used as the main power source for electric vehicles [4]. During rapid charge and discharge of lithium batteries, electrical energy, and chemical energy will be converted mu-

---

\*Corresponding author, e-mail: huyu@xhlab.cn

tually, and much heat will be generated, causing the battery temperature to rise rapidly [5]. The best operating temperature range of lithium batteries is 25-45 °C [6]. Once the battery temperature exceeds the optimal range and continues to overheat, the active material on the electrodes will peel off and the internal materials degrade [7]. Furthermore, an overheated battery can short-circuit and develops into a thermal runaway of the cell or even the pack, which can lead to a fire or even an explosion [8, 9]. Therefore, it is very necessary to design a practical and robust lithium battery thermal management system (BTMS) for the normal operation of electric vehicles [10-12].

Generally, BTMS are divided into four categories, such as air cooling strategy, liquid cooling strategy, phase change material (PCM), and heat pipe strategy, which have been studied by many scholars. Park *et al.* [13] designed an active PCM thermal management system and found that PCM coupled with liquid cooling can further significantly reduce the battery temperature. Tang *et al.* [14] compared the cooling performance of different liquid cooling plates and evaluated the influence of different coolant flow rates and discharge rates on battery temperature system. Hata *et al.* [15] developed a hybrid cooling system composed of heat pipes and PCM, and found that it can effectively reduce the high temperature caused by battery thermal runaway. Compared with other thermal management strategies, the air-cooling strategies have the advantages of low cost, simple structure, light weight and convenient design [16, 17]. Therefore, air-cooling strategies are widely used in electric vehicle thermal management systems, and researches on the structural design and parameter optimization of air-cooled battery packs have also attracted much attention. Jiaqiang *et al.* [18] explored the influence of different inlet positions on air cooling performance. A baffle is used to change the air-flow distribution inside the battery pack, which greatly improves the thermal performance of the battery pack. Feng *et al.* [19] designed a finned heat exchanger with secondary heat exchange characteristics for the air-cooled battery pack, which expanded the heat exchange process and improved the heat exchange efficiency. Xiaoming *et al.* [20] considered the transient thermal power of the longitudinal cell and studied the effects of three working conditions (continuous deceleration, continuous acceleration, and pulse discharge) on the temperature rise and temperature difference of the air-cooled battery pack. In order to meet the specification requirements, the battery temperature difference should be as small as possible [21]. However, most of the existing air-cooled battery module designs use a single air inlet and outlet, which may cause differences in cooling air-flow between batteries, and increase the temperature difference of the battery pack. Therefore, some scholars improve uniformity of the temperature in lithium-ion battery pack of electric vehicles by changing the battery arrangement or the position of the airway [18, 19], but the volume of the battery pack is increased and the volumetric energy density is reduced, which affects the energy economy of electric vehicles.

In this paper, a multi-inlet and multi-outlet battery pack consisting of 48 pieces of 18650 cylindrical batteries was studied. First, thermal-lumped treatment is applied to each cell in the module. Based on the measured experimental values, the transient heat generation of the battery is determined. Then, the temperature of the battery pack under different discharge rates and different cooling flow rate is numerically simulated to study the heat dissipation performance of the air-cooled system. Finally, the air-cooled system of the battery module was optimized by the comparative analysis of different battery configurations with different inlet area, outlet area, inlet spacing and outlet spacing, which provides the best optimization scheme for the heat dissipation performance of the battery module.

## Design descriptions

The simplified structure of the battery pack in this study is shown in fig. 1, which consists of 48 pieces of 18650 commercial lithium-ion batteries (the diameter of the battery is 18 mm and the height of the battery is 65 mm) with an electrical configuration is 8S6P (8 batteries in series and 6 batteries in parallel). The gap between the batteries is 2.5 mm decided by the structure of standard battery holder which is made of acrylonitrile butadiene styrene

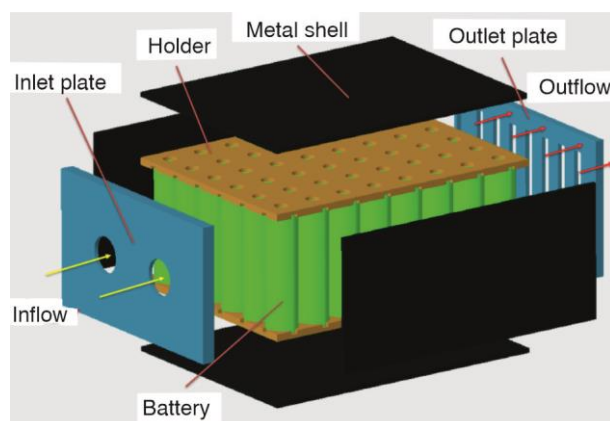


Figure 1. Simplified geometry of the battery pack

(ABS) plastic. There is a 20 mm gap between the top of the battery and the module shell, and a 10 mm gap between the battery and the shell in other directions for electric connections of battery management system (BMS). Consequently, the length, width, and height of the assembled battery pack are 192 mm, 151 mm, and 95 mm, respectively. The left side of the battery pack is the air inlet, while the right side is the air outlet. The air inlet is a circular surface, and the air outlet is a rectangular surface with a height of 65 mm, and its centre position is on the symmetrical plane

in the up-down direction. The outer surface of the battery is in contact with the air, so the heat dissipation of the battery is mainly through forced air convection. The temperature of the battery pack under different discharge rates and cooling flow rates is analysed to determine the configuration beyond the optimal temperature range of the battery. Then, the air inlet and outlet structure parameters are optimized to maximize the heat dissipation performance. The structural parameters taken for the analysis were are: the inlet diameter,  $D$ , the outlet width,  $W$ , spacing between inlets,  $\Delta L$ , and spacing between outlets  $\Delta W$ .

The parameters of the air inlet and the outlet are optimized separately. By fixing the values of the last two parameters, the first two parameters can be changed. Then with the optimal value of The first two parameters, the optimal value of the last two parameters is determined. Thermophysical properties of the structural components of the battery pack are list in tab. 1. These thermal physical parameters are constant values and regardless of the influence with time and temperature.

Table 1. Thermophysical properties of structural components of the battery pack

Parameter type	Holder	Pack shell	Air inlet and outlet plate
Density [ $\text{Kg m}^{-3}$ ]	1020	2170	1473
Specific heat capacity [ $\text{JKg}^{-1}\text{K}^{-1}$ ]	1390	880	1900
Thermal conductivity [ $\text{Wm}^{-1}\text{K}^{-1}$ ]	0.23	237	0.3

## Numerical model

### Lumped model for a single battery

The 18650 commercial lithium-ion battery consists of an anode current collector (copper foil), an anode electrode, a separator, a cathode electrode, and a cathode current col-

lector (aluminum foil). The thermophysical properties of each component are different. The internal area of the 18650 lithium battery is a multi-layer roll structure, which will cause a lot of computational cost. Therefore, a single battery is equivalent to a homogeneous cylinder, and the thermal-lumped treatment is used to determine the thermophysical properties of the equivalent battery structure to improve the calculation efficiency of the simulation and keep the accuracy of the results.

#### Heat generation rate of LIB used in simulation

Benardi *et al.*, [22] studied the heat generation mechanism of lithium batteries and summarized the heat generation model:

$$Q = Q_{ir} + Q_{re} = I^2 R + IT \frac{\partial E_o}{\partial T} \quad (1)$$

where  $Q$ ,  $Q_{ir}$ ,  $Q_{re}$  are the heat generation, the irreversible heat, and the reversible heat,  $I$  – the current,  $R$  – the internal resistance of the battery,  $T$  – the temperature of the battery, and  $\partial E_o / \partial T$  – the entropy weight coefficient. The heat generations of the single battery are affected by many factors and changes transiently. In this study, the heat generation of the battery during 1C, 3C, and 5C discharge is defined as a mathematical polynomial that varies with depth of discharge based on experimental measurements [23].

#### Governing equations

The CFD method is most commonly used to investigate the thermal behavior of the battery. It can simulate the temperature field and flow field in the battery pack under any operating conditions, which improve the efficiency of the analysis. The CFD analysis is based on energy conservation equation, continuity equation, and momentum equation. Any flowing object needs to follow the law of mass conservation and momentum conservation, which is presented as:

$$\frac{\partial \rho}{\partial t} + \nabla(\rho u) = 0 \quad (2)$$

$$\frac{\partial u}{\partial t} + (u \nabla) u = -\frac{\nabla p}{\rho} + \frac{\mu}{\rho} \nabla^2 u \quad (3)$$

where  $\rho$ ,  $\mu$ ,  $p$  are the density of the fluid, the dynamic viscosity, and pressure, respectively. There is a winding structure inside the battery, so it is assumed that the thermal conductivity is anisotropic. The energy conservation equation can be expressed as:

$$\rho C \frac{\partial T}{\partial t} = \left( k_x \frac{\partial^2 T}{\partial x^2} + k_y \frac{\partial^2 T}{\partial y^2} + k_z \frac{\partial^2 T}{\partial z^2} \right) + Q \quad (4)$$

where  $\rho$ ,  $C$ ,  $T$  are the density, heat capacity, and temperature of the battery, respectively,  $k_x$ ,  $k_y$ , and  $k_z$  – the constant thermal conductivity along the  $x$ -,  $y$ -, and  $z$ -directions, respectively, and  $Q$  – the heat generation of the battery.

#### Boundary/initial conditions and numerical strategy

The simulation type in this paper belonged to the conjugate coupling heat transfer of fluid and solid, so the heat loss caused by radiation is negligible. The density and viscosity of the fluid are assumed to be constant and do not change with time and temperature. Gravity

was not considered in this simulation. The air inlet is set as a mass-flow inlet, and the air temperature at the inlet is the same as the ambient temperature, which is set to 25 °C. The pressure at the air outlet is the same as the ambient pressure, and the relative pressure is 0 Pa. There is air around the battery pack, so the natural convection heat transfers between the battery pack and the air is considered, and the convective heat transfer coefficient is set to 5 W/mK. The inner wall surface of the battery pack is set to a no-slip boundary condition. The Reynolds number is small, so the laminar flow model is used in the calculation of the fluid domain.

### *Meshing and grid independence test*

The grid has an important impact on CFD transient simulation. In the meshing strategy, structured hexahedral grids are divided for cylindrical batteries and shells, while unstructured grids are divided for the complex fluid region to ensure boundary fitting. Data is transferred between unstructured and structured grids through the interface face. The meshing process was done in ANSY MESHING as shown in fig. 2.

The density of the grid will affect the accuracy of the calculation. The coarse grid will cause the calculation result distorted, and the fine grid will increase the computational cost. Therefore, under the same boundary conditions, three types of grids with different cell sizes are divided for grid independence test of grid number to determine the optimal grid configuration. The results are presented in fig. 3, it can be found that the maximum temperature difference within 2% when the grid number increase from 1.6 million to 2.8 million. Therefore, the grid configuration with 2.8 million grid number was adopted.

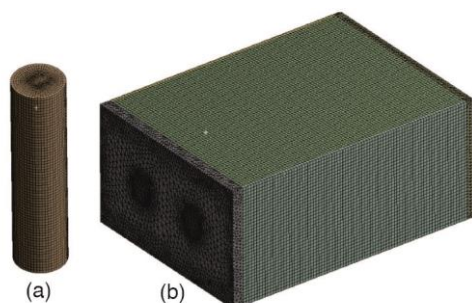


Figure 2. Mesh (a) and single cell (b) battery pack

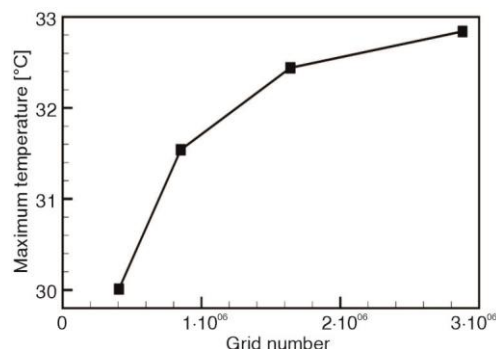


Figure 3. Grid independence test

## **Results and analysis**

### *Effect of discharge rate and flow rate*

Figure 4 explore the cooling performance of the battery pack with different flow rates and different discharge rates. The inlet flow rate is set to a sufficiently wide range of 0.18-1.72 Lps, and the battery discharge rates are set to 1C, 3C, and 5C. Figure 4(a) shows the comparison of the maximum temperature under different parameter configurations. It can be seen that the increase of the discharge rate caused the increase of the maximum temperature, while the increase of the cooling flow rate caused the decrease of the maximum temperature. Figure 4(b) shows the relationship between temperature difference and flow rate at three discharge rates. Similar to the analysis result of the maximum temperature, the battery pack un-

der the high discharge rate shows a larger temperature difference. When the battery discharge rate is increased to 5C, the maximum temperature of batteries exceeds the optimal range of 25-45 °C. By adjusting the inlet flow rate to 1.72 Lps, the maximum temperature of the battery is reduced to 42.15 °C and the temperature difference is reduced to 7.99 °C. Therefore, based on the 5C discharge rate and 1.72 Lps flow rate, the heat dissipation of the battery pack is further enhanced by adjusting other structural parameters.

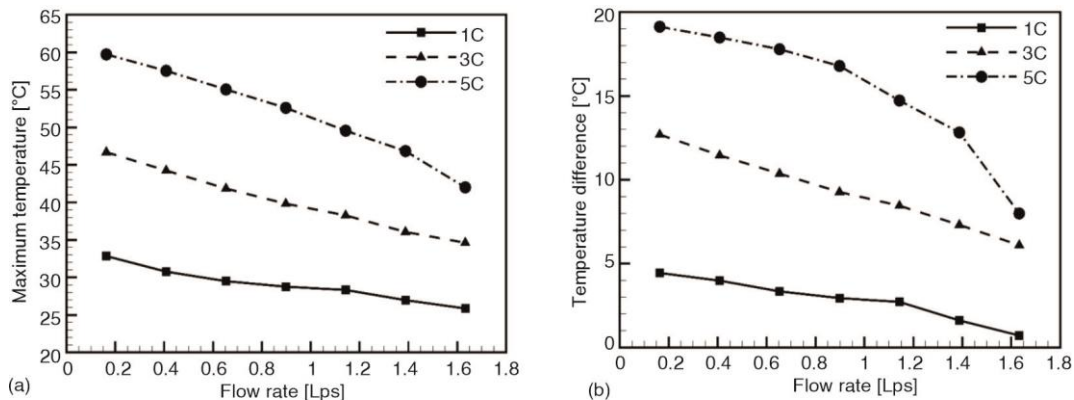


**Figure 4.** Comparison of different discharge rates and cooling flow rates;  
(a) maximum temperature and (b) temperature difference

#### *Effect of the area of air inlet and outlet*

In the structure of the air-cooled lithium battery pack, the air inlet and outlet play a role in controlling the air-flow. When the flow rate of the cooling air is fixed, the velocity of the cooling air is determined by the area of the air inlet and outlet, which will affect the cooling performance of the BTMS. Therefore, the effect of the air inlet and outlet area on the battery pack temperature is studied in this section. The area of the air inlet is related to the diameter,  $D$ , while the area of the air outlet is related to the width,  $W$ . The diameter,  $D$ , is changed from 10 mm to 30 mm, and the width,  $W$ , is changed from 2 mm to 10 mm. The results are presented in fig. 5.

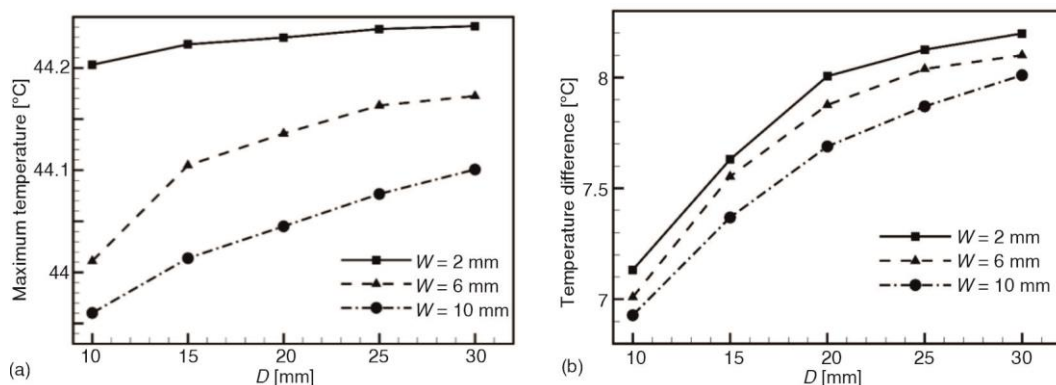


**Figure 5.** Comparison of different diameters,  $D$ , and widths,  $W$ ;  
(a) maximum temperature and (b) temperature difference

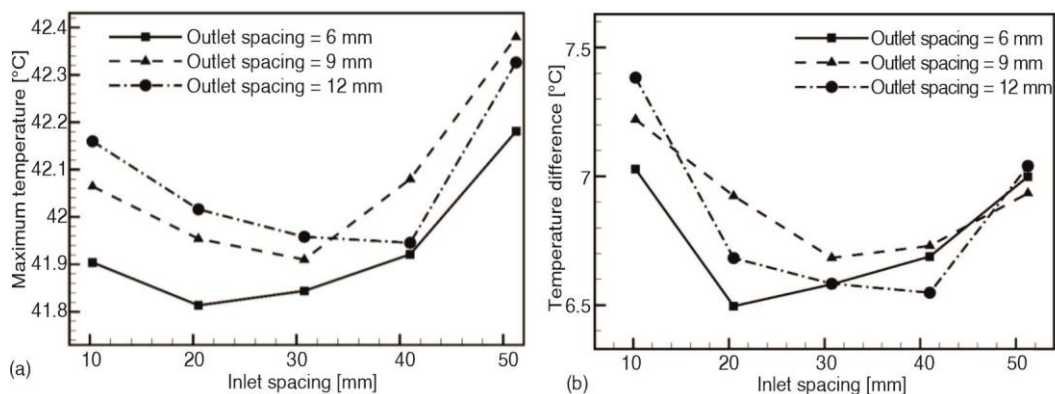


Figure 5(a) shows the maximum temperature and temperature difference of the battery pack with different inlet diameters and outlet widths, while fig. 5(b) shows the temperature difference of the module. As the diameters of the air inlet is increased from 10 mm to 30 mm, the values of the max temperature with a width of 6 mm were 42.01-42.17 °C. In fig. 5(b), the values of the temperature difference were 7.01-8.10 °C. In addition, the width of the outlet also affects the heat dissipation performance of the battery module. When the diameter,  $D$ , is 10 mm, by increasing the width, the maximum temperature of the battery pack is reduced from 42.20-41.96 °C. Meanwhile, the temperature difference is also reduced from 7.14-6.93 °C. The reason is that the increase in the outlet width is beneficial to the emission of hot air in the battery pack. Therefore, by comparing different schemes, it is determined that  $D = 10$  mm and  $W = 10$  mm are the best parameter configurations by comparing different schemes.

#### Effect of the spacing of air inlet and outlet

From section *Effect of the area of air inlet and outlet*, optimal area parameters of air inlet and outlet are obtained. In order to obtain a more uniform and lower battery pack temperature, it is very important to optimize the arrangement of the air inlet and outlet. The relative position of the inlet is determined by the spacing  $\Delta L$  between two inlets, while the relative positions of outlets is determined by the spacing  $\Delta W$ . The parameters  $\Delta L$  is changed from 10 mm to 40 mm, and the width  $\Delta W$  is changed from 6 mm to 9 mm. Figure 6 show the corresponding results.

Figure 6 presents the variation of the maximum temperature and temperature difference with different inlet spacing and outlet spacing. In fig. 6(a), for the case of outlet spacing  $\Delta W = 6$  mm, the maximum temperature of cells is reduced with the increase of inlet spacing  $\Delta L$ . However, as inlet spacing  $\Delta L$  exceeds 20.5 mm, the maximum temperature gradually increases. Figure 6(b) shows the temperature difference of the battery pack, the trend is similar to the maximum temperature. The results show that there is a different optimal inlet spacing for different air outlet spacing, so that the battery pack can obtain the optimal thermal performance. When inlet spacing is 20.5 mm and outlet spacing is 6 mm, the maximum temperature of the battery is reduced to 41.78 °C, and the temperature difference is reduced to 6.50 °C, which shows a best heat dissipation effect.



**Figure 6.** Comparison of different Inlet spacing,  $\Delta L$ , and outlet spacing,  $\Delta W$ ;  
 (a) maximum temperature and (b) temperature difference

### Comparison of heat dissipation performance

In order to demonstrate the effectiveness of multi-inlet and multi-outlet design, the temperature of the optimal multi-inlet and multi-outlet battery pack is compared with the single-inlet and single-outlet scheme. The flow rate is set to 1.72 Lps and the discharge rate is set to 5C. Figure 7 shows the temperature contour of the battery pack, and tab. 2 lists the maximum temperature and temperature difference of two battery packs. As shown in fig. 7, the battery temperature near the inlet side of multi-inlet and multi-outlet battery pack is lower and more uniform. Meanwhile, the temperature of the battery near the outlet side is reduced to within 41.78 °C. Compared with the single-inlet and single-outlet design, the maximum temperature of the multi-inlet and multi-outlet battery pack is reduced by 3.25 °C and the temperature difference was reduced by 3.14 °C, which show a better thermal performance of the battery pack.

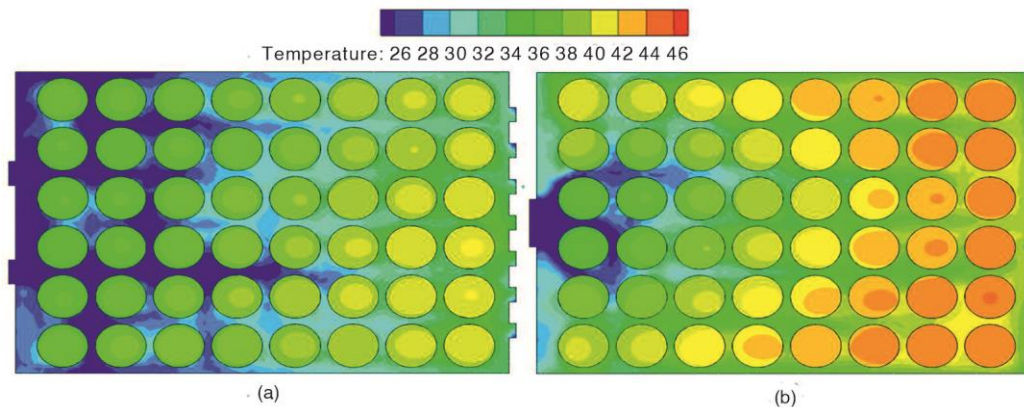


Figure 7. Comparison of temperature contour; (a) multi-inlet and multi-outlet and (b) single-inlet and single-outlet

Table 2. Comparison of different cooling schemes

Scheme	Maximum temperature [°C]	Temperature difference [°C]
Single-inlet and Single-outlet	45.03	9.64
Multi-inlet and Multi-outlet (not optimized)	42.15	7.99
Multi-inlet and Multi-outlet (optimized)	41.78	6.50

### Conclusion

In this study, a multi inlet and outlet air cooling-based battery module based is proposed. The effects of discharge rate, flow rate of the cooling air, the area of the air inlet and outlet the spacing of the air inlet and outlet are studied. The cooling performance of the battery pack is evaluated by monitoring the maximum temperature and temperature difference. Finally, the optimal parameter configuration of the heat dissipation performance was obtained for this study. The main conclusions are presented as follows.

- The maximum temperature and temperature difference of the battery pack will increase with the increase of the discharge rate. When the discharge rate reaches 5C, the battery pack will have a high temperature exceeding 45 °C. By increasing the inlet flow, the temperature of the battery pack can be effectively reduced.



- Considering that the velocity of the cooling fluid affect the heat exchange of the battery pack, the area of the air inlet and the air outlet is optimized to improve the heat dissipation performance. When the inlet diameter is 10 mm and the outlet width is 9 mm, a relatively lower value of the maximum temperature and temperature difference of the battery is obtained.
- The cooling performance of the battery pack can be further improved by optimizing the spacing of the inlet and outlet of the battery pack. When inlet spacing is 20.5 mm and outlet spacing is 6 mm, the best heat dissipation performance of the battery pack is obtained.
- Compared with the single-inlet and single-outlet designs, the multiple-inlet and multi-outlet scheme exhibit a lower and more uniform temperature distribution. The maximum temperature is relatively reduced by 3.25 °C, and the temperature difference is relatively reduced by 3.14 °C, which meets the requirements of battery temperature control.

## References

- [1] Vidadili, N., et al., Transition to Renewable Energy and Sustainable Energy Development in Azerbaijan, *Renewable and Sustainable Energy Reviews*, 80 (2017), Dec., pp. 1153-1161
- [2] Amjad, S., et al., Review of Design Considerations and Technological Challenges for Successful Development and Deployment of Plug-In Hybrid Electric Vehicles, *Renewable and Sustainable Energy Reviews*, 14 (2010), 3, pp. 1104-1110
- [3] Tie, S. F., Tan, C. W., A Review of Energy Sources and Energy Management System in Electric Vehicles, *Renewable and Sustainable Energy Reviews*, 20 (2013), Apr., pp. 82-102
- [4] Choi, H., Oh, I., Analysis of Product Efficiency of Hybrid Vehicles and Promotion Policies, *Energy Policy*, 38 (2010), 5, pp. 2262-2271
- [5] Bradley, T. H., Quinn, C. W., Analysis of Plug-In Hybrid Electric Vehicle Utility Factors, *Journal of Power Sources*, 195 (2010), 16, pp. 5399-5408
- [6] Pesaran, A. A., Battery Thermal Models for Hybrid Vehicle Simulations, *Journal of power sources*, 110 (2002), 2, pp. 377-382
- [7] Weng, J., et al., Alleviation of Thermal Runaway Propagation in Thermal Management Modules Using Aerogel Felt Coupled with Flame-Retarded Phase Change Material, *Energy Conversion and Management*, 200 (2019), Nov., 112071
- [8] Guo, Z., Chen, Z., High-Temperature Capacity Fading Mechanism for LiFePO<sub>4</sub>/Graphite Soft-Packed Cell without Fe Dissolution, *Journal of Electroanalytical Chemistry*, 754 (2015), Oct., pp. 148-153
- [9] Liu, W., et al., Improvement of the High-Temperature, High-Voltage Cycling Performance of LiNi<sub>0.5</sub>Co<sub>0.2</sub>Mn<sub>0.3</sub>O<sub>2</sub> Cathode with TiO<sub>2</sub> Coating, *Journal of Alloys and Compounds*, 543 (2012), Dec., pp. 181-188
- [10] Cicconi, P., et al. Virtual prototyping approach to evaluate the thermal management of Li-ion batteries, *Proceedings, IEEE Vehicle Power and Propulsion Conference (VPPC)*, Coimbra, Portugal, 2014, pp. 1-6
- [11] Gachot, G., et al., Thermal Behaviour of the Lithiated-Graphite/Electrolyte Interface through GC/MS Analysis, *Electrochimica Acta*, 83 (2012), Nov., pp. 402-409
- [12] Wang, T., et al., Thermal Investigation of Lithium-Ion Battery Module with Different Cell Arrangement Structures and Forced Air-Cooling Strategies, *Applied energy*, 134 (2014), Dec., pp. 229-238
- [13] Peng, X., et al., A Thermal Investigation and Optimization of an Air-Cooled Lithium-Ion Battery Pack, *Energies*, 13 (2020), 11, 2956
- [14] Tang, A., et al., Optimization Design and Numerical Study on Water Cooling Structure for Power Lithium Battery Pack, *Applied Thermal Engineering*, 159 (2019), Aug., 113760
- [15] Hata, H., et al., Performance Evaluation of a Battery-Cooling System using Phase-Change Materials and Heat Pipes for Electric Vehicles Under the Short-Circuited Battery Condition, *Journal of Thermal Science and Technology*, 13 (2018), 2, JTST0024-JTST0024
- [16] Giuliano, M. R., et al., Experimental Study of an Air-Cooled Thermal Management System for High Capacity Lithium-Titanate Batteries, *Journal of Power Sources*, 216 (2012), Oct., pp. 345-352
- [17] Wang, H., Ma, L., Thermal Management of a Large Prismatic Battery Pack Based on Reciprocating Flow and Active Control, *International Journal of Heat and Mass Transfer*, 115 (2017), A, pp. 296-303

- [18] Jiaqiang, E., *et al.*, Effects of the Different Air Cooling Strategies on Cooling Performance of a Lithium-Ion Battery Module with Baffle, *Applied Thermal Engineering*, 144 (2018), Nov., pp. 231-241
- [19] Feng, X., Hu, J., Analysis and Optimization Control of Finned Heat Dissipation Performance for Automobile Power Lithium Battery Pack, *Thermal Science*, 24 (2020), 5B, pp. 3405-3412
- [20] Xiaoming, X., *et al.*, Research on the Heat Dissipation Performance of Lithium-Ion Cell with Different Operating Conditions, *International Journal of Energy Research*, 41 (2017), 11, pp. 1642-1654
- [21] Park, H., A Design of Air Flow Configuration for Cooling Lithium Ion Battery in Hybrid Electric Vehicles, *Journal of power sources*, 239 (2013), Oct., pp. 30-36
- [22] Bernardi, D., *et al.*, A General Energy Balance For Battery Systems, *J. Electrochem. Soc.*, 132 (1985), 1, p. 5
- [23] Zhao, C., *et al.*, Thermal Behavior Study of Discharging/Charging Cylindrical Lithium-Ion Battery Module Cooled by Channeled Liquid Flow, *Int. J. Heat Mass Transf.*, 120 (2018), May, pp. 751-762